Ellagic Acid Mitigates Cadmium Exposure-Induced Apoptosis in HT22 Cells via Inhibiting Oxidative Stress, Mitochondrial Dysfunction, and Activating Nrf2/Ho-1 Pathway

Yue Liu , Chunhong Chen , Zhihui Hao , Jianzhong Shen , Shusheng Tang * , Chongshan Dai *

Posted Date: 11 September 2024

doi: 10.20944/preprints202409.0912.v1

Keywords: Cadmium; Ellagic acid; JNK pathway; Oxidative stress; Apoptosis; Nrf2/HO-1 pathway

Article

Ellagic Acid Reduces Cadmium Exposure-Induced Apoptosis in HT22 Cells via Inhibiting Oxidative Stress and Mitochondrial Dysfunction and Activating Nrf2/HO-1 Pathway

Yue Liu [1,2], Chunhong Chen [1,2], Zhihui Hao [1,2], Jianzhong Shen [1,2], Shusheng Tang [1,2,*] and Chongshan Dai [1,2,*]

[1] National Key Laboratory of Veterinary Public Health and Safety, College of Veterinary Medicine, China Agricultural University, Beijing, 100193, P.R. China
[2] Key Biology Laboratory of Chinese Veterinary Medicine, Ministry of Agriculture and Rural Affairs, Beijing, 100193, P.R. China
* Correspondence: tssfj@cau.edu.cn (S.T.); daichongshan@cau.edu.cn (C.D.)

Abstract: Exposure to cadmium sulfate ($CdSO_4$) can lead to neurotoxicity. Nevertheless, the precise molecular mechanisms underlying this phenomenon remain unclear, and effective treatment strategies are scarce. This study explored the protective effects of ellagic acid (EA), a natural polyphenolic compound, against $CdSO_4$ exposure-induced neurotoxicity in HT22 cells. Additionally, the investigation sought to elucidate the molecular mechanisms underlying this phenomenon. Our findings demonstrated that exposure of HT22 cells to $CdSO_4$ resulted in apoptosis, which was effectively reversed by EA supplementation. EA supplementation also decreased reactive oxygen species (ROS) and mitochondrial ROS productions, reduced malondialdehyde (MDA) levels, and restored the activities of superoxide dismutase (SOD) and catalase (CAT). Additionally, EA supplementation at 5–20 μM significantly counteracted Cd-induced mitochondrial membrane potential and ATP losses and reduced the ratio of Bax/Bcl-2 and cleaved-caspase-3 protein expression. Furthermore, EA supplementation upregulated Nrf2 and HO-1 protein expression while downregulating the phosphorylation of JNK and p38 proteins. Pharmacological inhibition of JNK partially inhibited $CdSO_4$-induced Nrf2/HO-1 activation and exacerbated its cytotoxicity. In conclusion, our results indicate that EA supplementation provides protection against $CdSO_4$-induced cell apoptosis in HT22 cells by inhibiting oxidative stress and activating the Nrf2 pathway. Activation of the JNK pathway plays a protective role in $CdSO_4$-induced cell apoptosis in HT22 cells.

Keywords: cadmium; ellagic acid; JNK pathway; oxidative stress; apoptosis; Nrf2/HO-1 pathway

1. Introduction

Cadmium (Cd) is a prevalent non-essential heavy metal known to have highly toxic effects on both humans and animals [1]. Cd has been ranked 7th in the hazardous waste priority list according to the U.S. Environmental Protection Agency's Superfund, based on its level of toxic risk [1]. The World Health Organization and The International Agency for Research on Cancer (IARC) have both classified Cd as a human carcinogen [2]. Previous studies from animal models and in vitro cell models showed that Cd exposure could cause multiple toxic effects, including hepatoxicity, nephrotoxicity, reproductive toxicity, immunotoxicity, and gastrointestinal toxicity [3–7]. Cd has the potential to penetrate the blood-brain barrier (BBB), leading to its accumulation in the central nervous system and ultimately causing neurotoxicity. A recent epidemiological investigation showed that environmental exposure to Cd may be a risk factor for Alzheimer's disease in humans [8]. In a mouse

 doi:10.20944/preprints202409.0912.v1

model, Cd exposure could result in the abnormal neurobehavioral changes (such as movement disorders, attention deficits, headaches and cognitive dysfunction) and pathological injury in brain tissues [9–11]. Hence, investigating the potential health risks of environmental Cd exposure in the nervous system and understanding the underlying molecular mechanisms are of great importance.

Currently, the precise molecular mechanisms of Cd exposure-induced neurotoxicity remain not fully understood. Deng et al. found that chronic exposure to Cd could result in cognitive function impairment in male mice by promoting mitochondrial fission and dysfunction of brain tissues [1]. It was reported that Cd exposure could affect the function of mitochondria via blocking the electron transport chain and decreasing membrane potential in neuronal cells in vitro [8,12]. A previous study found that Cd exposure at 2.5-20 μM could induce excessive production of reactive oxygen species (ROS) and decrease the abilities of the antioxidant defense system, triggering oxidative stress damage and mitochondrial dysfunction in PC12 cells and rat primary cerebral cortical neurons [13]. Moreover, it was also documented that Cd exposure could also trigger the activation of p53, sirtuin-1 (SIRT1), mitogen-activated protein kinase (MAPK), PKR-like ER kinase (PERK)/activating transcription factor 4 (ATF4), and ferroptosis pathways in neuronal cells and human peripheral blood lymphocytes [11,13–17].

Ellagic acid (EA) is a polyphenolic compound (2,3,7,8-tetrahydroxychromeno (5,4,3-cde) chromene-5,10-dione, C14H6O8; Figure 1) and it could be found in multiple gallnuts and fruits, such as pomegranates, black currants, raspberries, and mango [18]. Literature reports that EA exhibits various biological activities, such as anti-inflammatory, antiviral, antioxidant, antimicrobial, and immune-regulatory effects [19]. A mouse model showed that oral EA administration could effectively attenuate rotenone exposure-induced dopamine neuronal damage via targeting activation of Nrf2 pathway [20]. Goudarzi et al. study showed that oral EA supplementation at the doses of 10 and 30 mg/kg per day for successive twenty-one days can effectively attenuate sodium arsenate-caused neurotoxicity through inhibiting oxidative stress and neuroinflammation in the brain tissue of rats [21]. The current study aims to examine the protective effects of EA supplementation against Cd exposure-induced toxicity in HT22 cells, a mouse hippocampal neuronal cell line. Additionally, we explore the underlying molecular mechanisms.

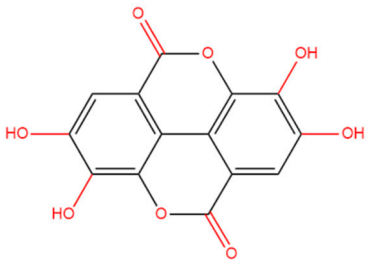

Figure 1. The structure of ellagic acid (2,3,7,8-tetrahydroxychromeno (5,4,3-cde) chromene-5,10-dione, C14H6O8).

2. Materials and Methods

2.1. Chemical and Reagents

Cadmium sulfate ($CdSO_4$) (purity ≥ 98%) and ellagic acid (purity more than 96%) were both purchased from Aladdin (Shanghai, China). SB203580 (a special inhibitor of p38 MAPK), SP600125 (a special inhibitor of JNK), dimethyl sulfoxide (DMSO), 1% (v/v) penicillin -streptomycin, phenylmethanesulfonylfluoride (PMSF), pan-caspase inhibitor (Z-VAD-FMK), and N-acetylcysteine (NAC) were provided by Beyotime Biotechnology Company (Haimen, Jiangsu, China). ASN007 (a special inhibitor of ERK) was purchased from MCE (Shanghai, China). Mito-TEMPO was purchased from Santa Cruz Biotechnology (Dallas, TX, USA). All other chemical regents used in the present study were at analysis grade.

 doi:10.20944/preprints202409.0912.v1

2.2. Cell Viability and Treatment

The mouse HT22 and rat PC12 cell lines were both obtained from the Shanghai Cell Bank of the Chinese Academy of Sciences (Shanghai, China). Cells were cultured in Dulbecco's Modified Eagle's Medium (DMEM) supplemented with 10% (v/v) fetal bovine serum (FBS) and 1% (v/v) penicillin-streptomycin under controlled conditions in a cell incubator at 5% CO_2 and 37 °C.

2.3. Measurement of Cell Viabilities

Cell viabilities were determined using a CCK-8 detection kit (Nanjing KeyGEN Biotech Co., Ltd, Nanjing, China), according to the instructions provided by the manufacturer. Briefly, A 96-well cell culture plate was used. 1×10^4 cells were seeded per well. After 24 hours cultivation, cells were treated with the various concentrations of $CdSO_4$ (0.625, 1.25, 2.5, 5, 10, 20, and 40 μM) or EA (5, 10, 20, 40, and 80 μM) for another 24 hours. After the treatment, cells were incubated with 10 μL of CCK-8 reagent for 1 hour. Then, cell viabilities were determined at 450 nm using a microplate reader (Tecan Trading AG, Kanton Zürich, Switzerland).

We also tested the effects of EA, antioxidant NAC, JNK inhibitor (i.e., SP600125) supplementation on Cd exposure-induced cytotoxicity in HT22 cells. In brief, cells were pre-treated with EA at the doses of 5, 10, and 20 μM, NAC at the dose of 2.5 mM, or JNK inhibitor at the dose of 10 μM, or SB203580 and ASN007 at the doses of 5 and 10 μM for 2 hours, then cells were co-treated with $CdSO_4$ at 10 μM for additional 24 hours. Finally, the cell viabilities were measured.

2.4. LDH Measurement

Shown in Supplementary Materials and Methods.

2.5. Measurement of Cell Apoptosis

Cell apoptosis analysis was performed using a commercial apoptosis analysis kit (Vazyme Biotech Co., Ltd., Nanjing, China) by flow cytometry analysis (Becton Dickinson, San Jose, CA, USA), according to the description in a previous study [22]. Meanwhile, the nuclear morphological changes were observed using the Hoechst 33342 staining method. Chromosome aggregation and the formation of apoptotic bodies are considered cell apoptosis and were counted.

2.6. Measurement of Intracellular ROS Levels and Oxidative Stress Biomarkers

Shown in Supplementary Materials and Methods.

2.7. Measurement of Mitochondrial ROS

The levels of mitochondrial ROS were measured using the MitoSOX staining method (M36008, Invitrogen), according to our previous study [23]. In brief, cells were pre-treated with EA at the dose of 20 μM or Mito-TEMPO for 2 hours, the co-treated with or without $CdSO_4$ at 10 μM for additional 24 hours. Then, cells were washed twice with PBS and incubated with MitoSOX Red (at 5 μM) plus 4′-6-diamidino-2-phenylindole (DAPI) for additional 30 min. Finally, cells were washed using PBS for twice and a laser confocal microscope (Leica Microsystems, Germany) was used.

2.8 Measurement of Intracellular ATP Levels

Shown in Supplementary Materials and Methods.

2.9. Western Blotting

The expression of proteins was analyzed using Western Blotting, according to the detailed protocol provided in a previous study [24]. The primary rabbit polyclonal antibodies against phosphorylated (p)-p38 (Thr180/Tyr182), p-JNK (Thr183/Tyr185), p-ERK1/2 (Thr202/Tyr204) (1:1000 dilution; CST company, Beverly, MA, USA), Nrf2, HO-1, Bax, Bcl-2, and caspase-3 (1:1000 dilution; Proteintech, Chicago, IL, USA), and mouse monoclonal antibody against β-actin (1:1000 dilution;

 doi:10.20944/preprints202409.0912.v1

Santa Cruz, CA, USA) were used. The anti-Total OXPHOS Cocktail antibody was purchased form Abcam (Shanghai, China). The detailed protocol is shown in the Supplementary Materials and Methods.

2.10. Statistical Analysis

All data were processed using GraphPad Prism 9.0 software. A nonlinear model-based model from GraphPad Prism 9.0 software was employed for the calculation of IC_{50}. All data were shown as means ± standard deviation (SD), unless specially stated. The differences between any two groups were performed under a Tukey's multiple comparison test of 1-way analysis of variance. A *P*-value < 0.05 was considered as considered statistically significant.

3. Results

3.1. EA Supplementation Attenuates $CdSO_4$-Induced Loss of Cell Viability and the Release of LDH in HT22 Cells

We first established the toxic model of $CdSO_4$ cytotoxicity in HT22 cells. The results showed that $CdSO_4$ treatment for 24 hours dose-dependently decreased cell viability in HT22 cells. As shown in Figure 2A, $CdSO_4$ exposure at the concentrations of 2.5, 5, 10, 20, and 40 μM for 24 hours reduced the cell viabilities to 86%, 77%, 65%, 33%, and 9% (all $P < 0.01$), respectively, and the half maximal inhibitory concentration (IC_{50}) was 12.4 μM. Additionally, we also assessed the toxic effects of EA. As shown in Figure 2B, EA treatment at 5–20 μM for 24 hours did not change the cell viabilities of HT22 cells, but at 40 and 80 μM, the cell viabilities were decreased to 85% and 61% (both $P < 0.01$), respectively, compared to the untreated cells. Therefore, the concentrations of EA at 5–20 μM in the following investigation were used. Then, EA treatment at 5–20 μM could effectively decreased $CdSO_4$-induced cytotoxicity in HT22 cells and it was in a dose-dependent manner. As shown in in Figure 2C, EA treatment at concentrations of 5, 10, and 20 μM increased the cell viabilities to 77%, 84%, and 92% (all $P < 0.01$), respectively, compared to 10 μM $CdSO_4$ group; increased the cell viabilities to 43%, 49%, and 59% (all $P < 0.01$), respectively, compared to 20 μM $CdSO_4$ group; and increased cell viabilities to 20%, 26% ($P < 0.01$), and 29% ($P < 0.01$), respectively, compared to 40 μM $CdSO_4$ group. Similarly, in PC12 cells, $CdSO_4$ exposure at 5 μM significantly decreased the cell viabilities to 56% ($P < 0.01$) and morphological changes, which was ameliorated by EA supplementation at the concentrations of 10 and 20 μM (Supplementary Figure S1). The corresponding cell viability increased to 66% and 74% ($P < 0.05$ or 0.01), respectively.

Additionally, the sub-IC_{50} concentration of $CdSO_4$ at 10 μM was used to investigated the potential mechanisms of EA. Correspondingly, $CdSO_4$ treatment at 10 μM for 24 hours could result in marked morphology changes, such as cell shrinkage and lysis. EA co-treatment could improve these changes (Supplementary Figure S2). We also assessed the levels of LDH releases caused by $CdSO_4$ exposure and the protective effects of EA. Compared to the control group, $CdSO_4$ exposure for 24 hours could dose-dependently induce the release of LDH in the medium. The levels of LDH in the 2.5, 5, and 10 μM $CdSO_4$ treatment groups were significantly increased to 2.2-, 3.7-, and 5.5-fold (all $P < 0.01$) (Figure 2D). Pre-treatment with EA at doses of 5, 10, and 20 μM significantly reduced LDH levels to 4.1-, 3.4-, and 1.7-fold (all $P < 0.01$), respectively, compared to the group treated with $CdSO_4$ only (Figure 2E). Treatment with EA alone at a concentration of 20 μM for 24 hours did not result in changes to the LDH levels of HT22 cells, compared to the untreated control group.

 doi:10.20944/preprints202409.0912.v1

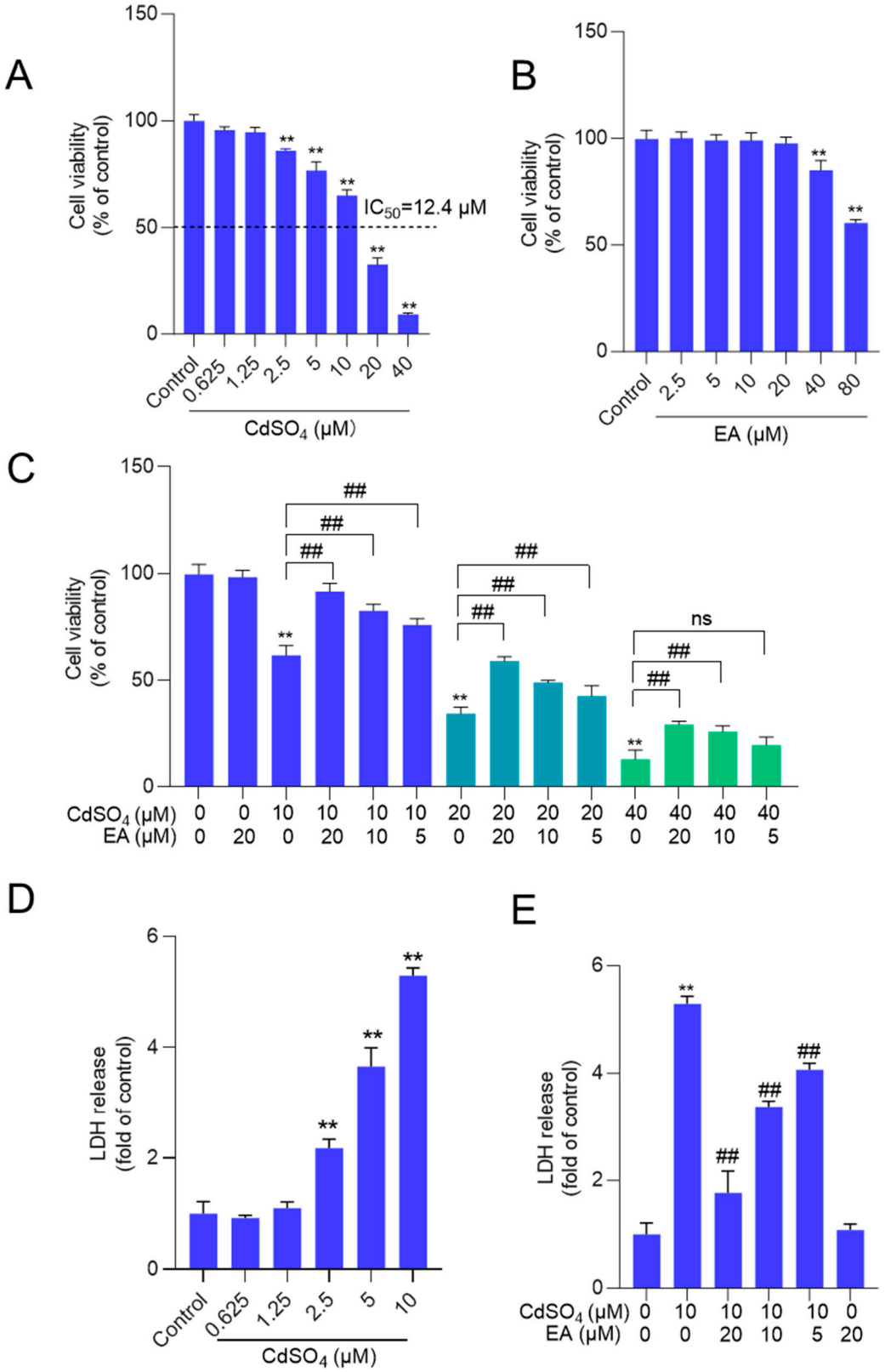

Figure 2. The cell viabilities and LDH levels in HT22 cells exposed to ellagic acid (EA), $CdSO_4$ or combination. A and B, cells were treated with $CdSO_4$ (at 0.625, 1.25, 2.5, 5, 10, 20, and 40 μM) (**A**) or EA at various concentrations (at 2.5, 5, 10, 20, and 40 μM) (**B**) for 24 hours, the cell viabilities were examined using the CCK-8 method. C, cells were pre-treated with EA at the doses of 5, 10, or 20 μM for 2 hours, then cells were co-treated with $CdSO_4$ at concentrations of 10, 20 or 40 μM for additional

 doi:10.20944/preprints202409.0912.v1

24 hours. After treatment, the cell viabilities were examined using the CCK-8 method. D and E, the levels of LDH in the medium. HT22 cells were treated with the same conditions as cells in A and B, respectively. All results were shown in mean ± SD (n = 3). Compared to the untreated control group, $^{**}P < 0.01$; compared to the $CdSO_4$ only-treated group, $^{\#\#}P < 0.01$.

3.2. *EA Supplementation Ameliorates $CdSO_4$-Induced Cell Apoptosis in HT22 Cells*

Exposure to CdSO4, when compared to the control group, resulted in significant changes in nuclear morphology. Figure 3A shows the presence of chromosomal aggregation and nuclear fragmentation in the 10 μM $CdSO_4$ treatment group, effects that were effectively reversed by pre-treatment with EA. Similarly, EA pre-treatment at doses of 5, 10, and 20 μM markedly prevented Cd-induced cell apoptosis, leading to a decrease in apoptotic rates from 29% to 20%, 12%, and 8% (all $P < 0.01$) respectively, compared to that in the 10 μM $CdSO_4$ only group (Figure 3B). Treatment with EA alone at a concentration of 20 μM for 24 hours did not result in alterations in apoptotic rates in HT22 cells compared to those in the untreated control group.

Similarly, we also found that Cd exposure at 5 μM increased the apoptosis rates to 43% ($P < 0.01$), compared to the control group. EA supplementation at 5, 10, and 20 μM decreased the apoptosis rates to 34%, 23%, and 17% (all $P < 0.01$), respectively (Suppl. Figure 3). EA supplementation at 20 μM for 24 hours did not affect the apoptosis rates in PC12 cells compared to the untreated control group (Supplementary Figure S3).

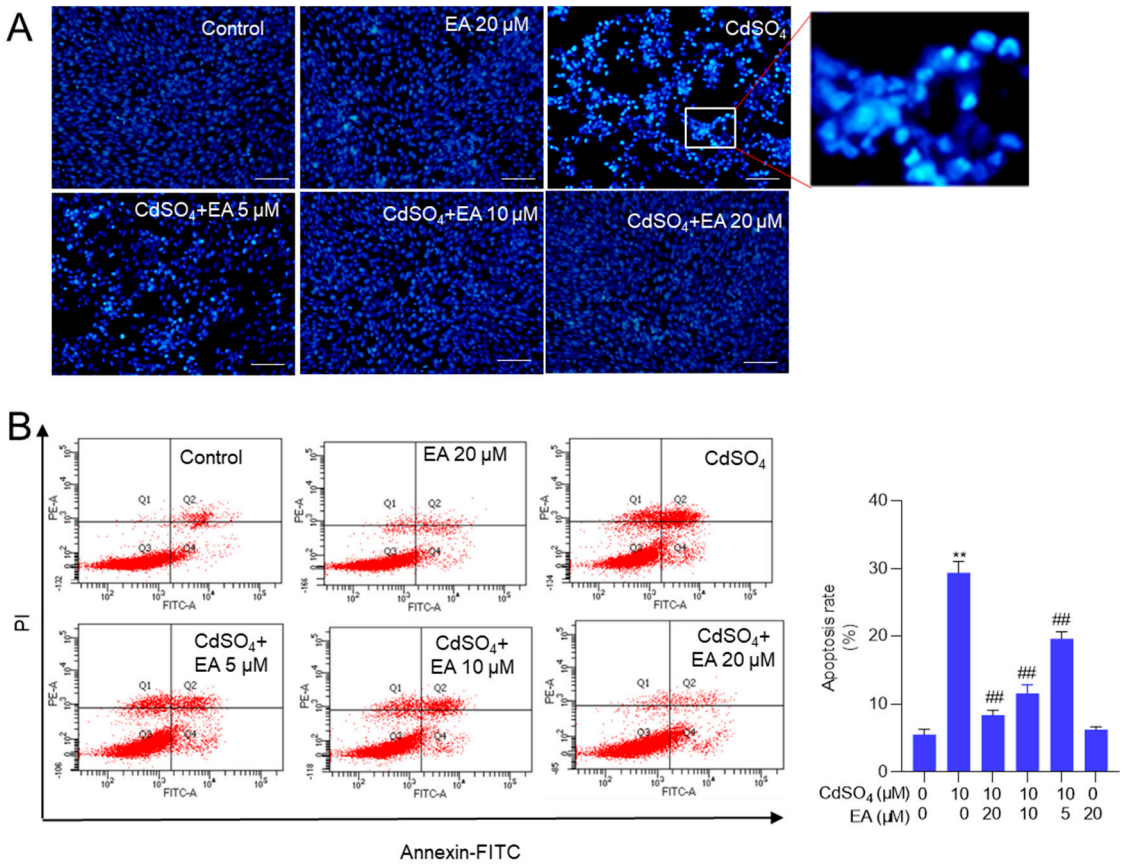

Figure 3. EA supplementation attenuates $CdSO_4$-induced cell apoptosis in HT22 cells. Cells were pre-treated with ellagic acid (EA) at final concentrations of 5, 10, or 20 μM for 2 hours, then co-treated with $CdSO_4$ at 10 μM for 24 hours. A, nuclear morphology changes were assessed using the Hoechst 33342 staining method. Bar = 50 μm. B, apoptotic rates were quantified through Annexin V-FITC staining combined with flow cytometry analysis. Representative images of the flow cytometry analysis (left) and quantitative results (right) are displayed. All data are presented as mean ± SD (n = 3). $^{**}P < 0.01$ compared to the control group; $^{\#\#}P < 0.01$ compared to the $CdSO_4$ only-treated group.

 doi:10.20944/preprints202409.0912.v1

3.3. EA Supplementation Attenuates $CdSO_4$-Induced ROS Production and Oxidative Stress Damage in HT22 Cells

Supplementary Figure S4A shows that the fluorescence intensities of DCFH-DA in HT22 cells treated with $CdSO_4$ alone were significantly heightened. This effect was partially alleviated by co-treatment with EA in a dose-dependent manner. A similar finding was also detected in PC12 cells (Supplementary Figure S4B). Then, the quantitative analysis using flow cytometry revealed a notable increase in fluorescence intensities to 46% in the 10 μM $CdSO_4$ treatment group in HT22 cells. Meanwhile, EA treatment at concentrations of 5, 10, and 20 μM led to significant reductions in fluorescence intensities to 30%, 26%, and 14% (all P <0.01), respectively, compared to the group solely treated with $CdSO_4$ (Figure 4A). Furthermore, the MitoSOX staining was performed. The results showed that the mitochondrial ROS levels were significantly increased to 2.6-fold, which were effectively decreased to 1.3- and 1.1-fold (both P < 0.01) by EA and Mito-TEMPO (shown in Supplementary Figure S5).

Additionally, the oxidative stress biomarkers, including MDA levels and the activities of SOD and CAT in HT22 cells, were evaluated. The results demonstrated that supplementation with EA effectively ameliorated Cd-induced oxidative damage. In Figure 4B–D, compared to the group exposed to 10 μM $CdSO_4$ only, treatment with EA at concentrations of 5, 10, and 20 μM notably reduced MDA levels from 0.85 nmol/mg protein to 0.65, 0.60, and 0.39 nmol/mg protein (all P < 0.01), respectively. Moreover, EA treatment significantly increased CAT activities from 2.1 U/mg protein to 3.3, 4.5, and 5.1 U/mg protein (all P < 0.05 or 0.01), respectively, and elevated SOD activities from 24.2 U/mg protein increased to 35.2, 41.3, and 51.5 U/mg protein (all P < 0.05 or 0.01). Notably, EA treatment at the concentration of 20 μM did not alter the levels of MDA or the activities of CAT and SOD compared to the control group (Figure 4B–D).

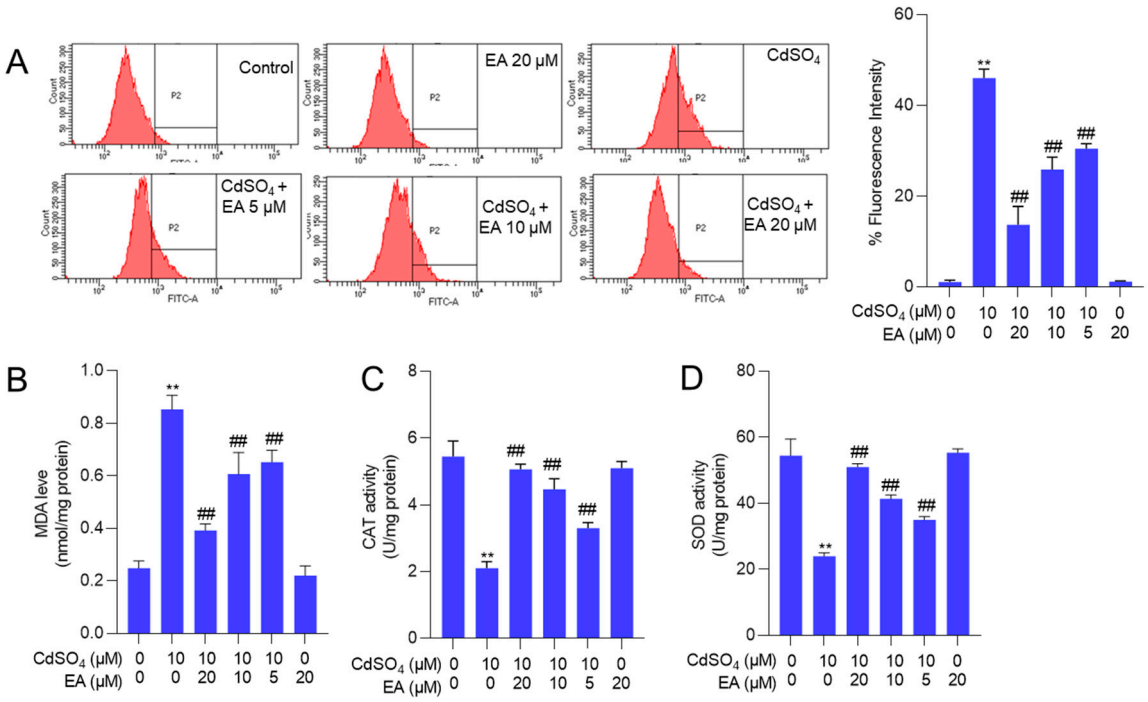

Figure 4. EA supplementation attenuates $CdSO_4$-induced ROS production and oxidative stress damage in HT22 cells. Cells were pre-treated with ellagic acid (EA) at 5, 10, or 20 μM for 2 hours, followed by co-treatment with $CdSO_4$ at a final concentration of 10 μM for 24 hours. A, the levels of reactive oxygen species (ROS) were assessed using DCFH-DA staining in conjunction with flow cytometry analysis, with representative images displayed (on the left) and quantitative analysis (on the right). B, malondialdehyde (MDA) levels. C, catalase (CAT) activities. D, The superoxide dismutase (SOD) activities. All results are presented as mean ± SD (n = 3). $^{**}P$ < 0.01 compared to that in the untreated control group; $^{\#\#}P$ < 0.01 compared to the $CdSO_4$ only-treated group.

 doi:10.20944/preprints202409.0912.v1

3.4. EA supplementation Attenuates $CdSO_4$-Caused Mitochondrial Dysfunction

Mitochondrial function was evaluated by measuring changes in mitochondrial membrane potential. In Figure 5A, EA treatment at concentrations of 5, 10, and 20 μM significantly increased the membrane potential from 56% to 70%, 81%, and 93% (all $P < 0.05$ or 0.01), respectively, compared to the group exposed to $CdSO_4$ alone. Subsequently, the protein expressions associated with the mitochondrial respiratory chain were assessed. Illustrated in Figure 5B, exposure to $CdSO_4$ led to a significant reduction in mitochondrial protein expressions of CI, CII, CIII, and CIV to 0.51-, 0.44-, 0.65-, and 0.52-fold (all P <0.05 or 0.01), respectively. The expression of the CV protein was unaffected. EA supplementation at 10 and 20 μM both effectively upregulated the protein expression of CI, II, and IV (all $P < 0.05$ or 0.01) compared to the group treated with $CdSO_4$ alone (Figure 5B). Consistently, we also found that $CdSO_4$ exposure significantly decreased the intracellular ATP levels to 46% ($P <$ 0.01) and EA supplementation at 10 and 20 μM both effectively restore the intracellular ATP levels to 89% and 92% (both $P < 0.01$) (Figure 5C). Additionally, EA treatment at a dose of 20 μM did not alter the mitochondrial membrane potential, the intracellular ATP levels, and the expression of CI, II, III, IV, and V compared to the untreated control group (Figure 5).

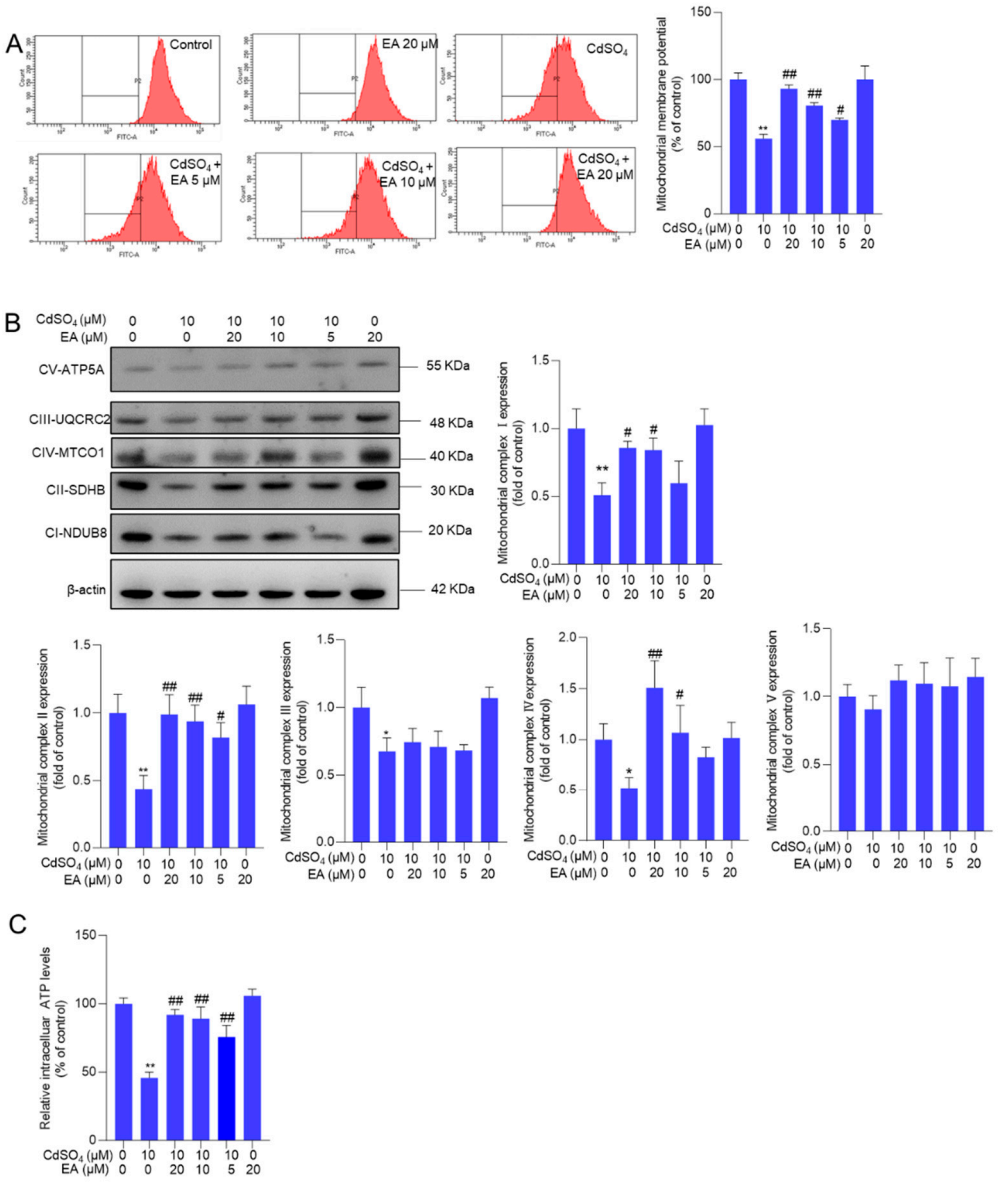

Figure 5. The changes in mitochondrial function. Cells were pre-treated with ellagic acid (EA) at 5, 10, or 20 μM for 2 hours, followed by co-treatment with $CdSO_4$ at 10 μM for an additional 24 hours.

 doi:10.20944/preprints202409.0912.v1

A, the changes in mitochondrial membrane potential were evaluated using Rh123 staining and flow cytometry analysis. The representative images (left) and quantitative analysis (right) were shown. B, the protein expression of mitochondrial complexes I-V was examined. C, the intracellular ATP levels. All results are presented as mean ± SD (n = 3). $^{**}P < 0.01$, compared to that in the untreated control group; $^{\#\#}P < 0.01$ compared to the $CdSO_4$ only-treated group.

3.5. EA Supplementation Upregulates the Expression of Nrf2, HO-1, and Bcl-2 Proteins and Downregulates the Expression of Bax, p-JNK, p-p38, and p-ERK Proteins

Compared to the untreated control group, exposure to 10 μM $CdSO_4$ significantly upregulated the expression of Nrf2, HO-1, p-Erk1/2, p-JNK, p-p38, Bax/Bcl-2 ratio, cleaved caspase-3, and cleaved PARP-1 proteins by 1.9-, 10.1-, 2.4-, 4.3-, 3.7-, 1.9-, 4.0-, and 2.6-fold, respectively (all $P < 0.01$) (Figure 6). These protein expressions were modulated by EA supplementation. Consistently, our results also found that caspase pan-inhibitor Z-VAD-FMK treatment at the dose of 20 μM could markedly inhibit $CdSO_4$-induced apoptosis (Supplementary Figure S6). EA supplementation at a dose of 20 μM plus $CdSO_4$ treatment significantly increased the expression of Nrf2 and HO-1 proteins by 3.1- and 16.3-fold, respectively, while notably decreasing the expression of p-Erk1/2, p-JNK, p-p38, Bax/Bcl-2 ratio, cleaved caspase-3, and cleaved PARP-1 proteins to 1.5-, 2.0-, 1.6-, 1.2-, 2.1-, and 1.0-fold (all $P < 0.01$; Figure 6), respectively.

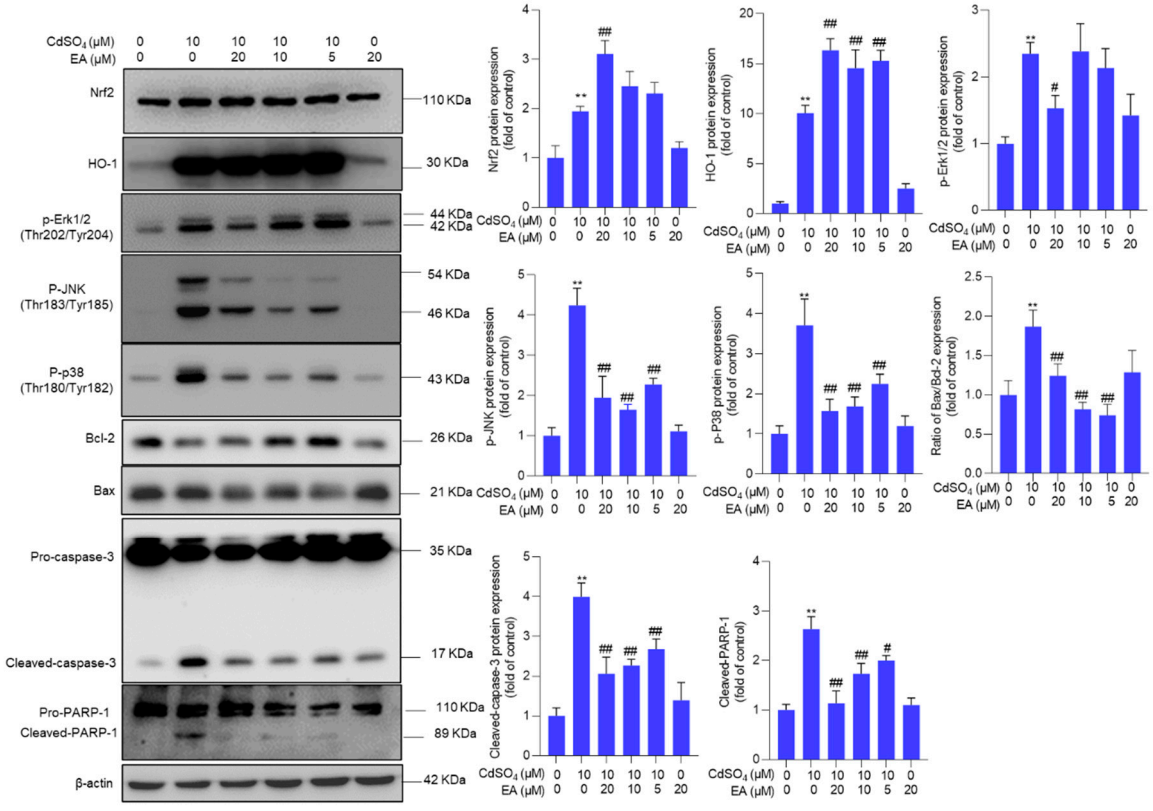

Figure 6. The expression of Nrf2, HO-1, p-Erk1/2, p-JNK, p-p38, Bax/Bcl-2 ratio, cleaved caspase-3, and cleaved PARP-1 proteins. Cells were pre-treated with ellagic acid (EA) at 5, 10, or 20 μM for 2 hours, followed by co-treatment with $CdSO_4$ at 10 μM for an additional 24 hours. Protein expressions were assessed using the Western Blotting method. All results were presented as Mean ± SD (n = 3). Statistical significance levels were delineated as follows: $^{**}P < 0.01$ compared to the untreated control group; $^{\#}P < 0.05$ and $^{\#\#}P < 0.01$ compared to the $CdSO_4$ only-treated group.

3.6. Pharmacological Inhibition of JNK Promotes $CdSO_4$-Induced Cytotoxicity

We further investigated the impact of the MAPK pathway on $CdSO_4$ exposure-induced cytotoxicity. We found that pharmacological inhibition of p38 and ERK pathway by SB203580 and

 doi:10.20944/preprints202409.0912.v1

ASN007 did not affect $CdSO_4$-induced cytotoxicity in HT22 cells (Supplementary Figure S7). However, pharmacological inhibition of JNK by SP600125 could significantly exacerbate $CdSO_4$ exposure-induced cytotoxicity (Figure 7A). Additionally, JNK inhibition led to a substantial decrease in the expression of Nrf2 and HO-1 proteins, which were decreased to 1.1- and 5.2-fold (both $P < 0.05$), respectively. On the contrary, compared to the group exposed to $CdSO_4$ only, JNK inhibition significantly increased the expression of the Bax/Bcl-2 ratio, cleaved caspase-3, and cleaved PARP-1 proteins to 2.4-fold ($P < 0.05$), 4.3-fold ($P < 0.01$), and 3.8-fold ($P < 0.05$) (Figure 7B).

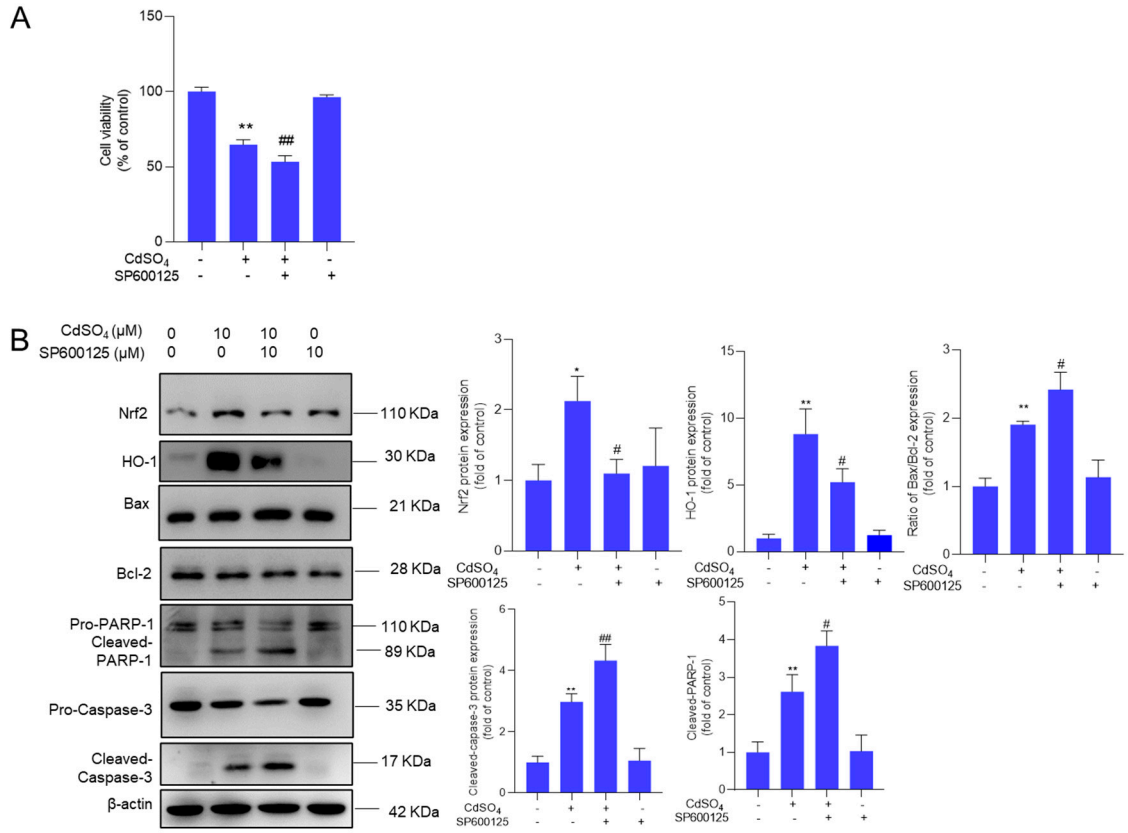

Figure 7. Pharmacological inhibition of JNK attenuates the activation of Nrf2/HO-1 and promotes $CdSO_4$ exposure-induced cytotoxicity. HT22 cells were treated with the JNK inhibitor SP600125 at 10 μM for 2 hours, then co-treated with $CdSO_4$ at 10 μM for an additional 24 hours. A, the changes in cell viability were assessed. B, the protein expressions were analyzed using the Western Blotting method. All results were presented as mean ± SD (n = 3). Significance levels were indicated as follows: $^{**}P < 0.01$ compared to the untreated control group; $^{\#}P < 0.05$, and $^{\#\#}P < 0.01$ compared to the $CdSO_4$ only-treated group.

3.7. NAC Supplementation Attenuates $CdSO_4$-Induced Cytotoxicity and the Activation of JNK and Mitochondrial Apoptotic Pathway

We confirmed the impact of oxidative stress on $CdSO_4$-induced cytotoxicity and the activation of the JNK and mitochondrial apoptotic pathways. Our findings indicated that supplementation with N-acetylcysteine (NAC) at a concentration of 2.5 mM effectively mitigated $CdSO_4$-induced ROS production (Supplementary Figure S8) and partially alleviated $CdSO_4$-induced cytotoxicity, resulting in an increase in cell viabilities from 61% to 90% ($P < 0.01$; Figure 8A). Additionally, NAC supplementation significantly attenuated the loss of mitochondrial membrane potential induced by $CdSO_4$ exposure (Figure 8B). Furthermore, NAC supplementation led to a substantial decrease in the expression of p-JNK, the Bax/Bcl-2 ratio, cleaved caspase-3, and cleaved PARP-1 proteins. In the NAC and $CdSO_4$ co-treatment group, the levels of p-JNK, the Bax/Bcl-2 ratio, cleaved caspase-3, and cleaved PARP-1 proteins nearly normalized, and they were decreased to 1.3-, 0.8-, 1.1-, and 1.1-fold

 doi:10.20944/preprints202409.0912.v1

(all $P < 0.01$) (Figure 8C), respectively. When compared to the control group, treatment with NAC alone did not affect cell viabilities, mitochondrial membrane potential, or the expression of the aforementioned proteins (Figure 8).

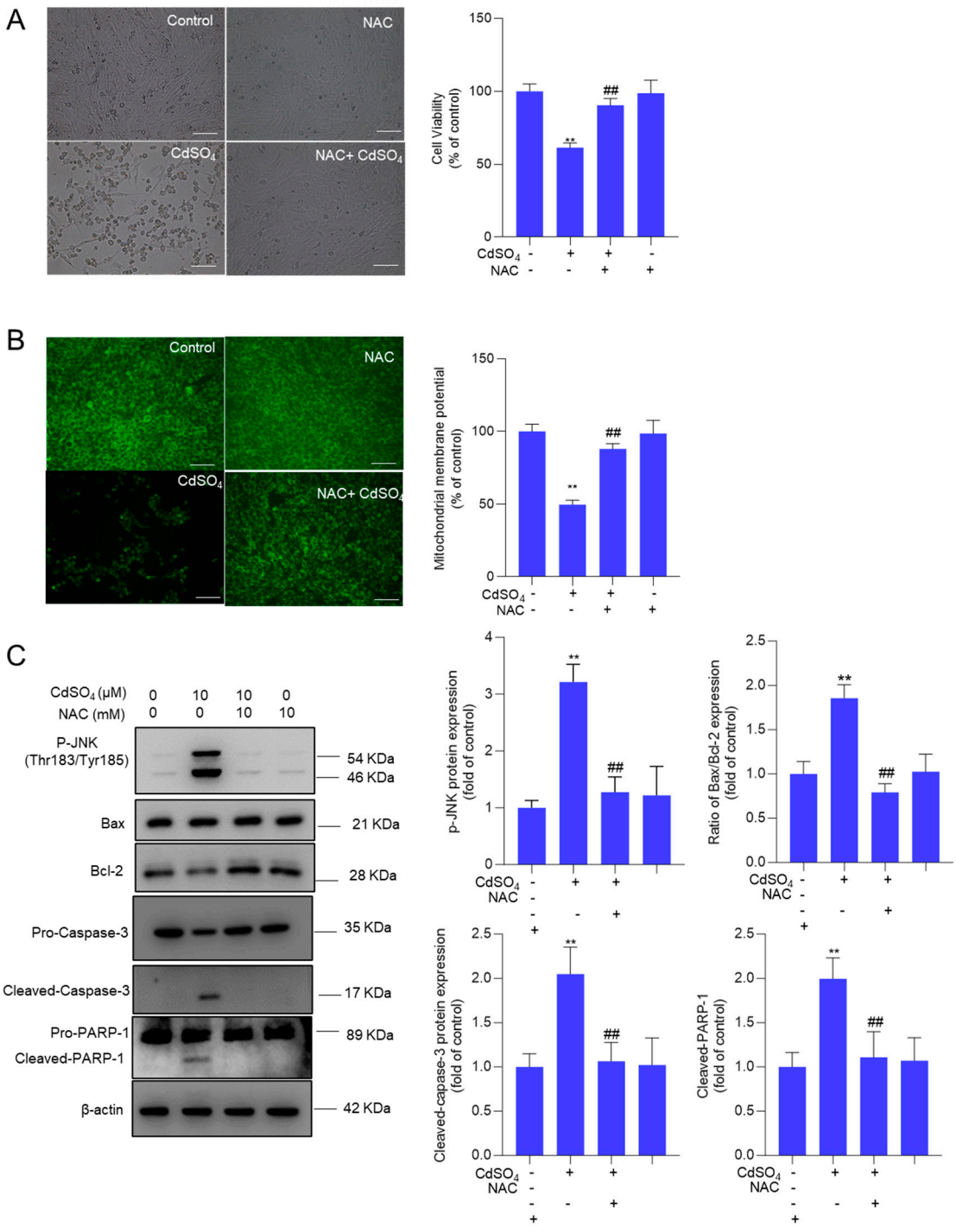

Figure 8. NAC supplementation attenuates $CdSO_4$-induced cytotoxicity and the activation of JNK and mitochondrial apoptotic pathway. Cells were treated with N-acetylcysteine (NAC) at a final concentration of 2.5 mM for 2 hours, followed by co-treatment with $CdSO_4$ at a final concentration of 10 μM for 24 hours. A, the cell morphology changes (left) and cell viability (right) were shown. Bar = 50 μm. B, the alterations in mitochondrial membrane potential, featuring representative images (left) and quantitative analysis (right). C, the protein expressions were assessed using the Western Blotting method. Data were presented as mean ± SD (n = 3). $^{**}P < 0.01$, compared to the untreated control group; $^{\#}P < 0.05$, and $^{\#\#}P < 0.01$, compared to the $CdSO_4$ only-treated group.

 doi:10.20944/preprints202409.0912.v1

4. Discussion

Neurotoxicity is one of multiple toxic effects caused by $CdSO_4$ exposure [16]. Previous studies demonstrated that $CdSO_4$ exposure at the range of 0.625–20 μM could induce marked decreases of cell viabilities in PC12 cells and HT22 cells [11,25]. Consistent with a previous study [11], our current study reveals that exposure to $CdSO_4$ at concentrations ranging from 0.625 to 40 μM resulted in dose-dependent cell death in HT22 cells. Previous studies have reported that the different test methods have the different sensitivity to Cd-induced cytotoxicity [26]. One non-negligible reason is that some heavy metals can affect the sensitivity of CCK-8 detection, and it might be increased with the increase of heavy metal concentration. In the present study, we used two methods, i.e., the CCK-8 and LDH methods, to assess the cytotoxicity and the protective effects of EA. Our results found that the LDH method is more sensitive than the CCK-8 method in Cd-treated HT22 cells（Figure 2). Meanwhile, we found that both two methods both demonstrated that the protective effects of EA on Cd-induced cytotoxicity (Figure 2). Similarly, EA supplementation at 5–20 μM could provide a protection against Cd-induced cytotoxicity in PC12 cells (Supplementary Figure S1). Furthermore, we observed a dose-dependent inhibition by EA supplementation on $CdSO_4$ exposure-induced oxidative stress, cell apoptosis, and mitochondrial dysfunction. These effects may be linked to EA's ability to scavenge free radicals, enhance antioxidant defense function, inhibit the JNK pathway, and activate the Nrf2/HO-1 pathway (Figures 3–8 and Supplementary Figures 3–8).

Apoptosis, a form of programmed cell death, can be induced by various drugs or environmental toxins, such as copper, cisplatin, and T-2 toxin [24,27–29] . In this study, we observed that exposure to $CdSO_4$ could initiate cell apoptosis (Figure 3), consistent with prior research [30,31]. Furthermore, our findings revealed that EA supplementation effectively ameliorated $CdSO_4$-induced cell apoptosis in HT22 and PC12 cells (Figure 3 and Supplementary Figure S3). Several previous studies demonstrated that EA supplementation can reduce drugs or toxins-induced apoptotic cell death in vitro and in vivo [32–34]. These findings suggest that EA's protective effects against $CdSO_4$-induced cytotoxicity involve the inhibition of apoptosis.

Apoptotic cell death could be triggered by multiple signals, including ROS, p53, and other apoptosis-related factors [24,35]. A prior study demonstrated that exposure to $CdSO_4$ can induce excessive ROS production, leading to direct damage to intracellular macromolecules (such as DNA, lipids, and proteins) and subcellular organelles (such as mitochondria, endoplasmic reticulum, and lysosomes), ultimately culminating in cell apoptosis [36]. Our current findings reveal that $CdSO_4$ exposure significantly elevates intracellular ROS and MDA levels while simultaneously decreasing the activities of SOD and CAT in HT22 cells (Figure 4). We also found that $CdSO_4$ exposure could significantly upregulate the mitochondrial ROS levels (Supplementary Figure S5). Similarly, Hyun et al. showed that Cd exposure at 10-40 μM for 24 hours could significantly upregulate the mitochondrial ROS levels in human prostate stromal cells and mouse embryonic fibroblasts [37]. These data suggested that $CdSO_4$ exposure-induced the excessive production is partly dependent on the production of mitochondrial ROS. SOD and CAT, as antioxidant enzymes, play crucial roles in combating oxidative stress by scavenging intracellular superoxide and hydroxyl radicals [26]. Increased MDA levels serve as an essential indicator of membrane lipid peroxidation [25]. These results indicate that $CdSO_4$ exposure elicits oxidative stress damage in HT22 cells. Notably, EA supplementation effectively attenuates $CdSO_4$-induced ROS and mitochondrial ROS productions and enhances SOD and CAT activities (Figure 4 and Supplementary Figure S5). Previous studies by Firdaus et al. demonstrated that EA pre-treatment at 10–20 μM can inhibit ROS production and apoptosis induced by arsenic trioxide in human neuroblastoma SH-SY5Y cells [38]. Similarly, Ding et al. reported that EA treatment at 15–30 μM reduces ROS production and MDA levels caused by high glucose exposure while improving SOD activities in HepG2 cells [39]. Moreover, Zhao et al. showed that EA supplementation at doses of 50–100 mg/kg/day for four weeks upregulates antioxidant enzymes, including CAT, SOD, and GSH-PX, to ameliorate ethanol exposure-induced liver injury in a mouse model [40]. Collectively, these findings suggest that EA supplementation effectively reduces $CdSO_4$-induced apoptosis by alleviating oxidative stress and mitochondrial ROS production. Furthermore, our study found that the expression of mitochondrial respiratory chain

 doi:10.20944/preprints202409.0912.v1

proteins CI, CII, CIII, and CIV and ATP production were significantly decreased after $CdSO_4$ exposure, indicating mitochondrial dysfunction (Figure 5). The inhibition of complexes I and II could induce the ROS generation [41,42]. Interestingly, EA supplementation alleviates $CdSO_4$-induced inhibition of CI, CII, and CIV proteins, as observed in our study (Figure 5) and supported by Khodaei et al.'s findings of EA's protective effect against cuprizone exposure-induced loss of CII, CIII, and CIV proteins in mouse muscle tissue [43]. In addition, our results also showed that EA treatment could effectively restore $CdSO_4$ exposure-induced the loss of intracellular ATP (Figure 5). It is known that mitochondrial respiration mainly relies on the enzymatic activities of five mitochondrial complexes that couple electron transport with proton pumping, finally leading to ATP synthesis [44]. Several previous studies also reported that Cd is a potent uncoupling agent and can inhibit mitochondrial respiratory chain activities by interacting with CI at Q site and NADH site and CI, CII, and CIII at Fe–S cluster [12,45–47]. These data suggest that EA's inhibition of ROS and mitochondrial ROS production resulting from $CdSO_4$ exposure may partly depend on its modulation on the expressions or activities of CI, CII, and CIV. Mitochondrial complexes could be regulated by several factors, the transcription coactivator peroxisome proliferator-activated receptor-γ (PPARγ) coactivator 1α (PGC1α), mTOR, and endoplasmic reticulum stress signaling [48]. Previous studies also demonstrated that Cd exposure could disturb disrupt the expression of PGC1α, mTOR, and the homeostasis of mitochondrial dynamics [49,50]. It is not clear that the expression co mitochondrial complexes and the modulation of EA whether are associated with these factors. Further investigation is warranted to elucidate the underlying molecular mechanisms.

Mitochondria serve not only as producers but also as targets of ROS [51]. Bax, a pro-apoptotic protein, contrasts with Bcl-2, an anti-apoptotic protein [51]. The mitochondrial membrane potential assessment stands as a pivotal indicator of mitochondrial dysfunction [24]. Deng et al. observed a significant loss of mitochondrial membrane potential in N2a neuronal cells upon exposure to cadmium chloride ($CdCl_2$) [1]. The elevation in the Bax/Bcl-2 ratio can instigate mitochondrial dysfunction, triggering the release of CytC and subsequently activating caspases-9 and -3 in a cascading fashion, culminating in cell apoptosis [52]. Poly (ADP-ribose) polymerase-1 (PARP-1) acts as a target of activated caspases-3 in caspase-dependent apoptosis, with cleaved PARP-1 suppressing DNA repair and serving as a key marker of apoptosis [53]. Our study demonstrates that $CdSO_4$ exposure notably diminishes mitochondrial membrane potential, leading to an increase in the Bax/Bcl-2 ratio, ultimately resulting in the upregulation of cleaved caspase-3 and cleaved PARP-1 protein expression (Figures 5 and 6). Pan-caspase inhibitor could markedly revise $CdSO_4$ -induced cell apoptosis (Supplementary Figure S6), indicating that $CdSO_4$-induced apoptotic cell death is caspase-dependent. EA supplementation partially reduces these $CdSO_4$-induced alterations (Figures 5 and 6). Furthermore, our data reveals that the antioxidant NAC supplementation significantly attenuates $CdSO_4$-induced cytotoxicity by suppressing ROS production and the mitochondrial apoptotic pathway (Supplementary Figure S8 and Figure 8). Therefore, these findings suggest that EA supplementation could effectively safeguard against $CdSO_4$-induced apoptosis by hindering mitochondrial dysfunction and the mitochondrial apoptotic pathway in HT22 cells, potentially attributable to its role in oxidative stress modulation.

Nrf2, a crucial transcription factor often referred to as a "housekeeper," responds to oxidative stress and inflammatory damage [54,55]. Studies have highlighted that Nrf2 activation exerts a protective effect against Cd-induced cytotoxicity and tissue damage [56,57]. Consistent with prior findings, our study demonstrated a significant upregulation of Nrf2 expression and its downstream gene HO-1 following $CdSO_4$ exposure, with further enhancements observed upon co-treatment with EA (Figure 6). Recent research has underscored Nrf2 as a vital target of EA, showing that EA promotes nuclear Nrf2 expression by inhibiting Keap1 expression [58]. Notably, Nrf2 knockout partially attenuated the protective effects of EA against rotenone-induced neurotoxicity in a mouse model [20]. Our current data strongly suggest that Nrf2 activation contributes to the EA-mediated protection against $CdSO_4$-induced apoptosis.

Previous studies have shown that Cd exposure can promptly activate the MAPK pathway, leading to a significant upregulation of p-Erk1/2, p-JNK, and p-p38 proteins in various cell types,

 doi:10.20944/preprints202409.0912.v1

including PC12 and SH-SY5Y neuronal cells and human bronchial epithelial cells (BEAS-2B) [59–61]. In these cell models, researchers observed that the inhibition of p-Erk1/2 and p-JNK partially attenuated Cd exposure-induced cell apoptosis [59–61]. Conversely, Liu et al. reported that inhibiting JNK did not influence Cd exposure-induced cell death in BmE cells, a silkworm embryonic cell line [62]. Given its diverse functions, the MAPK pathway typically exhibits a dual role in regulating cell apoptosis [63]. For instance, Hu et al. demonstrated that JNK-mediated activation of the Nrf2 pathway contributed to the protective effects of coptisine against 2,2'-azodiisobutyramidine dihydrochloride-induced oxidative stress damage in zebrafish embryos [63]. In the present study, we observed that JNK inhibition, not p38 and ERK inhibition, could promote $CdSO_4$-induced cytotoxicity at 24 hours (Supplementary Figure S7). Moreover, JNK inhibition by SP600125 markedly suppresses the expression of Nrf2 and HO-1 proteins, consequently exacerbating the mitochondrial apoptotic pathway and ultimately exacerbating $CdSO_4$ exposure-induced cell death (Figure 7). We also found that indicated that blocking oxidative stress with NAC substantially inhibited JNK activation (Figure 8 and Supplementary Figure S8), suggesting that oxidative stress is a crucial upstream regulator of the JNK pathway in $CdSO_4$-induced cytotoxicity. For the MAPK pathway, the time profile of activation is usually responsible for the biological outcome. In the current study, we just tested the effects of the MAPK pathway on $CdSO_4$-induced cytotoxicity at 24 hours. The dynamic changes of the MAPK pathway in response to $CdSO_4$ and how it mediates the protective effects of EA are still unknown. This is a limitation of the present study.

Importantly, EA has a higher safety for humans and animals and has been used in food production as a food additive [64,65]. Various studies indicate that EA supplementation could provide a neuroprotection for drugs or environmental toxins-induced neurotoxicity [20,34,66,67]. Taken together, these findings suggest that EA may be a potential protective agent against Cd-induced neurotoxicity, and further commercial development could be considered.

5. Conclusions

In summary, our results demonstrate that EA supplementation effectively reduced $CdSO_4$-induced cytotoxicity in HT22 cells by inhibiting oxidative stress and apoptosis, potentially via the activation of the Nrf2/HO-1 pathway. Additionally, the activation of the JNK pathway in response to $CdSO_4$ exposure also confers protection via the Nrf2/HO-1 pathway. A proposed model illustrating the impact of EA supplementation on $CdSO_4$-induced apoptosis is presented in Figure 9. This study highlights EA as a promising candidate for combating Cd-induced cytotoxicity and neurotoxicity.

 doi:10.20944/preprints202409.0912.v1

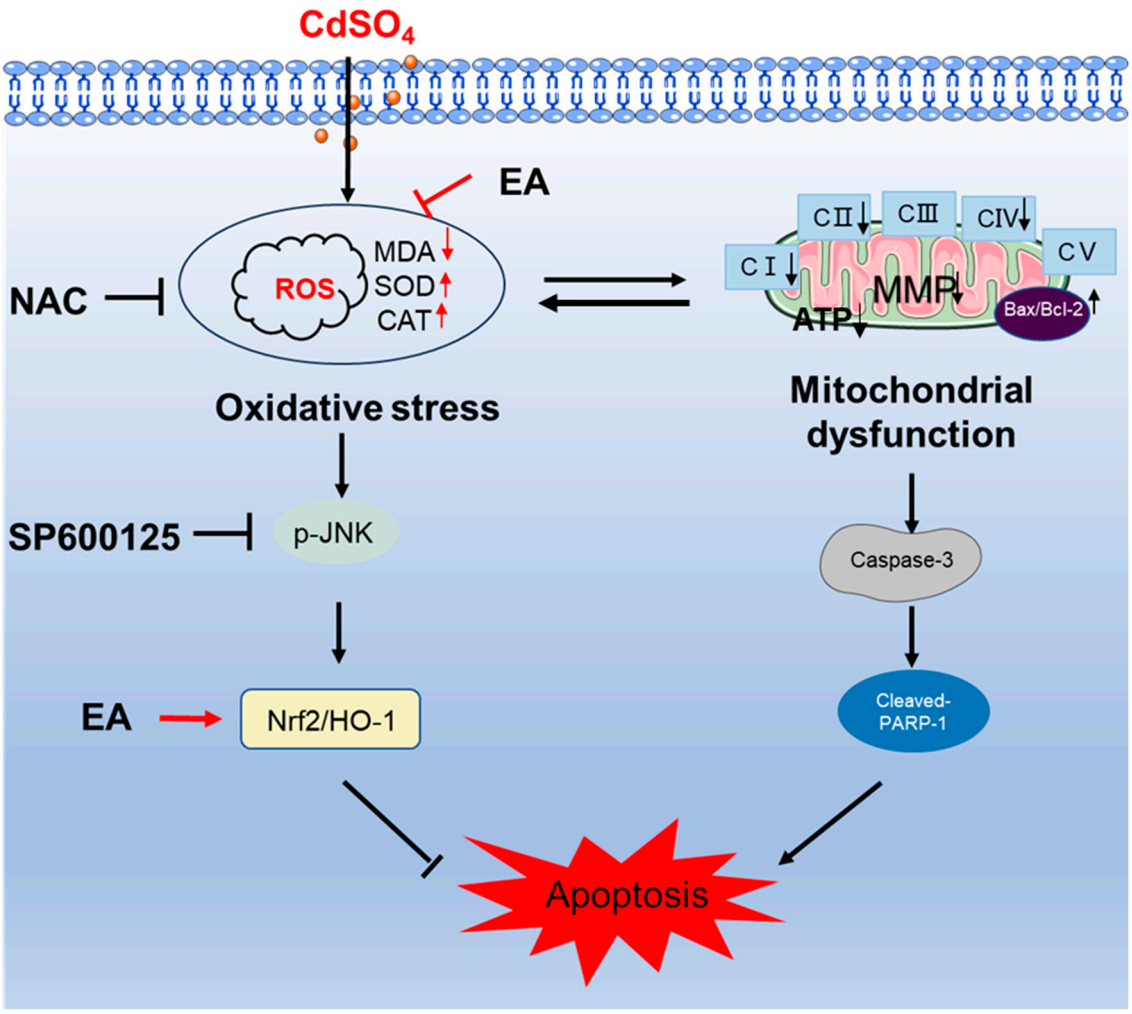

Figure 9. A potential proposed model of EA supplementation on $CdSO_4$ exposure-caused apoptosis. $CdSO_4$ exposure leads to the generation of reactive oxygen species (ROS) and lipid peroxidationwhile reducing the activities of antioxidant enzymes SOD and CAT, resulting in oxidative stress damage. Elevated ROS levels may disrupt mitochondrial function, triggering the activation of the mitochondrial apoptotic pathway and eventually culminating in apoptosis. Furthermore, activated JNK exerts a protective effect by stimulating the Nrf2/HO-1 pathway.

Supplementary Materials: The following supporting information can be downloaded at the website of this paper posted on Preprints.org. Suppl. Figure S1 The morphology changes (left) and the results of cell viabilities (right) in PC12 cells after $CdSO_4$ treatment with or without EA. Suppl. Figure S2 The morphology changes of HT22 cells after $CdSO_4$ treatment with or without EA. Suppl. Figure S3 EA supplementation attenuates $CdSO_4$-induced cell apoptosis in PC12 cells. Suppl. Figure S4 Representative images of DCFH-DA staining in HT22 cells (A) and PC12 cells (B). Suppl. Figure S5 Levels of mitochondrial ROS in HT22 cells. Suppl. Figure S6 Pan-caspase inhibitor Z-VAD-FMK suppresses $CdSO_4$ exposure-induced apoptosis. Suppl. Figure S7 Effects of pharmacological inhibition of p38 (A) and ERK (B) pathways by SB203580 and ASN007 on $CdSO_4$ exposure-induced cytotoxicity. Suppl. Figure S8 Antioxidant NAC supplementation attenuates $CdSO_4$-induced the production of intracellular ROS.

Author Contributions: Investigation, Y.L., and C.C.; data curation, Y.L., and C.C., and Z.H.; writing-original draft preparation, Y.L., and C.C., and C.D.; methodology, Y.L., C.D., and S.T.; formal analysis, Y.L., C.D., and S.T.; validation, Y.L., C.D., and S.T.; writing—review and editing, C.D., and J.S.; supervision, C.D.. All authors have read this final submitted version carefully and approved it.

Funding: This study was funded by the National Natural Science Foundation of China (Award number 32102724). This study was also funded by the Pinduoduo-China Agricultural University Research Fund (Grant No. PC2023A01002).

Institutional Review Board Statement: Not applicable.

Informed Consent Statement: Not applicable.

Data Availability Statement: The data are contained within the article and Supplementary materials.

Conflict of interest: The authors declared no conflicts of interest in the present study.

References

1. Deng, P.; Zhang, H.; Wang, L.; Jie, S.; Zhao, Q.; Chen, F.; Yue, Y.; Wang, H.; Tian, L.; Xie, J.; et al. Long-term cadmium exposure impairs cognitive function by activating lnc-Gm10532/m6A/FIS1 axis-mediated mitochondrial fission and dysfunction. *Sci Total Environ* **2023**, *858*, 159950. https://doi.org/10.1016/j.scitotenv.2022.159950.
2. Wang, M.; Chen, Z.; Song, W.; Hong, D.; Huang, L.; Li, Y. A review on Cadmium Exposure in the Population and Intervention Strategies Against Cadmium Toxicity. *Bulletin of environmental contamination and toxicology* **2021**, *106*, 65-74. https://doi.org/10.1007/s00128-020-03088-1.
3. Tinkov, A.A.; Gritsenko, V.A.; Skalnaya, M.G.; Cherkasov, S.V.; Aaseth, J.; Skalny, A.V. Gut as a target for cadmium toxicity. *Environmental pollution (Barking, Essex : 1987)* **2018**, *235*, 429-434. https://doi.org/10.1016/j.envpol.2017.12.114.
4. Xie, D.; Yan, J.; Zhang, H.; Zhang, H.; Nie, G.; Zhu, X.; Li, X. Cadmium exacerbates liver injury by remodeling ceramide metabolism: Multiomics and laboratory evidence. *Sci Total Environ* **2024**, *923*, 171405. https://doi.org/10.1016/j.scitotenv.2024.171405.
5. Zhao, C.; Yu, D.; He, Z.; Bao, L.; Feng, L.; Chen, L.; Liu, Z.; Hu, X.; Zhang, N.; Wang, T.; et al. Endoplasmic reticulum stress-mediated autophagy activation is involved in cadmium-induced ferroptosis of renal tubular epithelial cells. *Free radical biology & medicine* **2021**, *175*, 236-248. https://doi.org/10.1016/j.freeradbiomed.2021.09.008.
6. Qu, Z.; Liu, L.; Wu, X.; Guo, P.; Yu, Z.; Wang, P.; Song, Y.; Zheng, S.; Liu, N. Cadmium-induced reproductive toxicity combined with a correlation to the oogenesis process and competing endogenous RNA networks based on a Caenorhabditis elegans model. *Ecotoxicology and environmental safety* **2023**, *268*, 115687. https://doi.org/10.1016/j.ecoenv.2023.115687.
7. Wang, Z.; Sun, Y.; Yao, W.; Ba, Q.; Wang, H. Effects of Cadmium Exposure on the Immune System and Immunoregulation. *Front Immunol* **2021**, *12*, 695484. https://doi.org/10.3389/fimmu.2021.695484.
8. Min, J.Y.; Min, K.B. Blood cadmium levels and Alzheimer's disease mortality risk in older US adults. *Environmental health : a global access science source* **2016**, *15*, 69. https://doi.org/10.1186/s12940-016-0155-7.
9. Wang, H.; Abel, G.M.; Storm, D.R.; Xia, Z. Adolescent cadmium exposure impairs cognition and hippocampal neurogenesis in C57BL/6 mice. *Environmental toxicology* **2022**, *37*, 335-348. https://doi.org/10.1002/tox.23402.
10. Wang, H.; Zhang, L.; Abel, G.M.; Storm, D.R.; Xia, Z. Cadmium Exposure Impairs Cognition and Olfactory Memory in Male C57BL/6 Mice. *Toxicological sciences : an official journal of the Society of Toxicology* **2018**, *161*, 87-102. https://doi.org/10.1093/toxsci/kfx202.
11. Wang, D.; Wu, Y.; Zhou, X.; Liang, C.; Ma, Y.; Yuan, Q.; Wu, Z.; Hao, X.; Zhu, X.; Li, X.; et al. Cadmium exposure induced neuronal ferroptosis and cognitive deficits via the mtROS-ferritinophagy pathway. *Environmental pollution (Barking, Essex : 1987)* **2024**, *349*, 123958. https://doi.org/10.1016/j.envpol.2024.123958.
12. Branca, J.J.V.; Pacini, A.; Gulisano, M.; Taddei, N.; Fiorillo, C.; Becatti, M. Cadmium-Induced Cytotoxicity: Effects on Mitochondrial Electron Transport Chain. *Frontiers in cell and developmental biology* **2020**, *8*, 604377. https://doi.org/10.3389/fcell.2020.604377.
13. Wen, S.; Xu, M.; Zhang, W.; Song, R.; Zou, H.; Gu, J.; Liu, X.; Bian, J.; Liu, Z.; Yuan, Y. Cadmium induces mitochondrial dysfunction via SIRT1 suppression-mediated oxidative stress in neuronal cells. *Environmental toxicology* **2023**, *38*, 743-753. https://doi.org/10.1002/tox.23724.
14. Khan, A.; Ikram, M.; Muhammad, T.; Park, J.; Kim, M.O. Caffeine Modulates Cadmium-Induced Oxidative Stress, Neuroinflammation, and Cognitive Impairments by Regulating Nrf-2/HO-1 In Vivo and In Vitro. *Journal of clinical medicine* **2019**, *8*. https://doi.org/10.3390/jcm8050680.
15. Chandler, J.D.; Wongtrakool, C.; Banton, S.A.; Li, S.; Orr, M.L.; Barr, D.B.; Neujahr, D.C.; Sutliff, R.L.; Go, Y.M.; Jones, D.P. Low-dose oral cadmium increases airway reactivity and lung neuronal gene expression in mice. *Physiological reports* **2016**, *4*. https://doi.org/10.14814/phy2.12821.

16. Al Olayan, E.M.; Aloufi, A.S.; AlAmri, O.D.; El-Habit, O.H.; Abdel Moneim, A.E. Protocatechuic acid mitigates cadmium-induced neurotoxicity in rats: Role of oxidative stress, inflammation and apoptosis. *Sci Total Environ* **2020**, *723*, 137969. https://doi.org/10.1016/j.scitotenv.2020.137969.
17. Al-Assaf, A.H.; Alqahtani, A.M.; Alshatwi, A.A.; Syed, N.A.; Shafi, G.; Hasan, T.N. Mechanism of cadmium induced apoptosis in human peripheral blood lymphocytes: the role of p53, Fas and Caspase-3. *Environmental toxicology and pharmacology* **2013**, *36*, 1033-1039. https://doi.org/10.1016/j.etap.2013.09.006.
18. Kim, D.H.; Sim, Y.; Hwang, J.H.; Kwun, I.S.; Lim, J.H.; Kim, J.; Kim, J.I.; Baek, M.C.; Akbar, M.; Seo, W.; et al. Ellagic Acid Prevents Binge Alcohol-Induced Leaky Gut and Liver Injury through Inhibiting Gut Dysbiosis and Oxidative Stress. *Antioxidants (Basel)* **2021**, *10*. https://doi.org/10.3390/antiox10091386.
19. Gupta, A.; Singh, A.K.; Kumar, R.; Jamieson, S.; Pandey, A.K.; Bishayee, A. Neuroprotective Potential of Ellagic Acid: A Critical Review. *Advances in nutrition (Bethesda, Md.)* **2021**, *12*, 1211-1238. https://doi.org/10.1093/advances/nmab007.
20. Wei, Y.Z.; Zhu, G.F.; Zheng, C.Q.; Li, J.J.; Sheng, S.; Li, D.D.; Wang, G.Q.; Zhang, F. Ellagic acid protects dopamine neurons from rotenone-induced neurotoxicity via activation of Nrf2 signalling. *J Cell Mol Med* **2020**, *24*, 9446-9456. https://doi.org/10.1111/jcmm.15616.
21. Goudarzi, M.; Amiri, S.; Nesari, A.; Hosseinzadeh, A.; Mansouri, E.; Mehrzadi, S. The possible neuroprotective effect of ellagic acid on sodium arsenate-induced neurotoxicity in rats. *Life sciences* **2018**, *198*, 38-45. https://doi.org/10.1016/j.lfs.2018.02.022.
22. Dai, C.; Ciccotosto, G.D.; Cappai, R.; Tang, S.; Li, D.; Xie, S.; Xiao, X.; Velkov, T. Curcumin Attenuates Colistin-Induced Neurotoxicity in N2a Cells via Anti-inflammatory Activity, Suppression of Oxidative Stress, and Apoptosis. *Mol Neurobiol* **2018**, *55*, 421-434. https://doi.org/10.1007/s12035-016-0276-6.
23. Dai, C.; Li, M.; Sun, T.; Zhang, Y.; Wang, Y.; Shen, Z.; Velkov, T.; Tang, S.; Shen, J. Colistin-induced pulmonary toxicity involves the activation of NOX4/TGF-β/mtROS pathway and the inhibition of Akt/mTOR pathway. *Food Chem Toxicol* **2022**, *163*, 112966. https://doi.org/10.1016/j.fct.2022.112966.
24. Li, M.; Tang, S.; Velkov, T.; Shen, J.; Dai, C. Copper exposure induces mitochondrial dysfunction and hepatotoxicity via the induction of oxidative stress and PERK/ATF4 -mediated endoplasmic reticulum stress. *Environmental pollution (Barking, Essex : 1987)* **2024**, *352*, 124145. https://doi.org/10.1016/j.envpol.2024.124145.
25. Ben, P.; Zhang, Z.; Xuan, C.; Sun, S.; Shen, L.; Gao, Y.; Cao, X.; Zhou, Y.; Lan, L.; Yin, Z.; et al. Protective Effect of L-Theanine on Cadmium-Induced Apoptosis in PC12 Cells by Inhibiting the Mitochondria-Mediated Pathway. *Neurochemical research* **2015**, *40*, 1661-1670. https://doi.org/10.1007/s11064-015-1648-4.
26. Fotakis, G.; Timbrell, J.A. In vitro cytotoxicity assays: comparison of LDH, neutral red, MTT and protein assay in hepatoma cell lines following exposure to cadmium chloride. *Toxicology letters* **2006**, *160*, 171-177. https://doi.org/10.1016/j.toxlet.2005.07.001.
27. Chen, J.; Chu, Y.; Cao, J.; Yang, Z.; Guo, X.; Wang, Z. T-2 toxin induces apoptosis, and selenium partly blocks, T-2 toxin induced apoptosis in chondrocytes through modulation of the Bax/Bcl-2 ratio. *Food Chem Toxicol* **2006**, *44*, 567-573. https://doi.org/10.1016/j.fct.2005.09.004.
28. Liu, J.; Wang, L.; Guo, X.; Pang, Q.; Wu, S.; Wu, C.; Xu, P.; Bai, Y. The role of mitochondria in T-2 toxin-induced human chondrocytes apoptosis. *PLoS One* **2014**, *9*, e108394. https://doi.org/10.1371/journal.pone.0108394.
29. Mokhtari, Z.; Seyedhashemi, E.; Eftekhari, M.; Ghasemi, S.; Sabouri, A.; Abbaszadeh-Goudarzi, K.; Abuali, M.; Azimi, H.; Kesharwani, P.; Pourghadamyari, H.; et al. Enhancement of cisplatin-induced apoptosis by saffron in human lung cancer cells. *Journal of trace elements in medicine and biology : organ of the Society for Minerals and Trace Elements (GMS)* **2023**, *79*, 127229. https://doi.org/10.1016/j.jtemb.2023.127229.
30. Wang, T.; Yan, L.; Wang, L.; Sun, J.; Qu, H.; Ma, Y.; Song, R.; Tong, X.; Zhu, J.; Yuan, Y.; et al. VPS41-mediated incomplete autophagy aggravates cadmium-induced apoptosis in mouse hepatocytes. *Journal of hazardous materials* **2023**, *459*, 132243. https://doi.org/10.1016/j.jhazmat.2023.132243.
31. Yi, L.; Shang, X.J.; Lv, L.; Wang, Y.; Zhang, J.; Quan, C.; Shi, Y.; Liu, Y.; Zhang, L. Cadmium-induced apoptosis of Leydig cells is mediated by excessive mitochondrial fission and inhibition of mitophagy. *Cell Death Dis* **2022**, *13*, 928. https://doi.org/10.1038/s41419-022-05364-w.
32. Arab, H.H.; Gad, A.M.; Fikry, E.M.; Eid, A.H. Ellagic acid attenuates testicular disruption in rheumatoid arthritis via targeting inflammatory signals, oxidative perturbations and apoptosis. *Life sciences* **2019**, *239*, 117012. https://doi.org/10.1016/j.lfs.2019.117012.

33. Aslan, A.; Hussein, Y.T.; Gok, O.; Beyaz, S.; Erman, O.; Baspinar, S. Ellagic acid ameliorates lung damage in rats via modulating antioxidant activities, inhibitory effects on inflammatory mediators and apoptosis-inducing activities. *Environ Sci Pollut Res Int* **2020**, *27*, 7526-7537. https://doi.org/10.1007/s11356-019-07352-8.
34. Ardah, M.T.; Eid, N.; Kitada, T.; Haque, M.E. Ellagic Acid Prevents α-Synuclein Aggregation and Protects SH-SY5Y Cells from Aggregated α-Synuclein-Induced Toxicity via Suppression of Apoptosis and Activation of Autophagy. *Int J Mol Sci* **2021**, *22*. https://doi.org/10.3390/ijms222413398.
35. Dai, C.; Li, J.; Tang, S.; Li, J.; Xiao, X. Colistin-induced nephrotoxicity in mice involves the mitochondrial, death receptor, and endoplasmic reticulum pathways. *Antimicrob Agents Chemother* **2014**, *58*, 4075-4085. https://doi.org/10.1128/aac.00070-14.
36. Luo, H.; Gu, R.; Ouyang, H.; Wang, L.; Shi, S.; Ji, Y.; Bao, B.; Liao, G.; Xu, B. Cadmium exposure induces osteoporosis through cellular senescence, associated with activation of NF-κB pathway and mitochondrial dysfunction. *Environmental pollution (Barking, Essex : 1987)* **2021**, *290*, 118043. https://doi.org/10.1016/j.envpol.2021.118043.
37. Hyun, M.; Kim, H.; Kim, J.; Lee, J.; Lee, H.J.; Rathor, L.; Meier, J.; Larner, A.; Lee, S.M.; Moon, Y.; et al. Melatonin protects against cadmium-induced oxidative stress via mitochondrial STAT3 signaling in human prostate stromal cells. *Communications biology* **2023**, *6*, 157. https://doi.org/10.1038/s42003-023-04533-7.
38. Firdaus, F.; Zafeer, M.F.; Waseem, M.; Anis, E.; Hossain, M.M.; Afzal, M. Ellagic acid mitigates arsenic-trioxide-induced mitochondrial dysfunction and cytotoxicity in SH-SY5Y cells. *Journal of biochemical and molecular toxicology* **2018**, *32*. https://doi.org/10.1002/jbt.22024.
39. Ding, X.; Jian, T.; Wu, Y.; Zuo, Y.; Li, J.; Lv, H.; Ma, L.; Ren, B.; Zhao, L.; Li, W.; et al. Ellagic acid ameliorates oxidative stress and insulin resistance in high glucose-treated HepG2 cells via miR-223/keap1-Nrf2 pathway. *Biomed Pharmacother* **2019**, *110*, 85-94. https://doi.org/10.1016/j.biopha.2018.11.018.
40. Zhao, L.; Mehmood, A.; Soliman, M.M.; Iftikhar, A.; Iftikhar, M.; Aboelenin, S.M.; Wang, C. Protective Effects of Ellagic Acid Against Alcoholic Liver Disease in Mice. *Front Nutr* **2021**, *8*, 744520. https://doi.org/10.3389/fnut.2021.744520.
41. Okoye, C.N.; Koren, S.A.; Wojtovich, A.P. Mitochondrial complex I ROS production and redox signaling in hypoxia. *Redox Biol* **2023**, *67*, 102926. https://doi.org/10.1016/j.redox.2023.102926.
42. Dröse, S. Differential effects of complex II on mitochondrial ROS production and their relation to cardioprotective pre- and postconditioning. *Biochim Biophys Acta* **2013**, *1827*, 578-587. https://doi.org/10.1016/j.bbabio.2013.01.004.
43. Khodaei, F.; Rashedinia, M.; Heidari, R.; Rezaei, M.; Khoshnoud, M.J. Ellagic acid improves muscle dysfunction in cuprizone-induced demyelinated mice via mitochondrial Sirt3 regulation. *Life sciences* **2019**, *237*, 116954. https://doi.org/10.1016/j.lfs.2019.116954.
44. Vercellino, I.; Sazanov, L.A. The assembly, regulation and function of the mitochondrial respiratory chain. *Nature reviews. Molecular cell biology* **2022**, *23*, 141-161. https://doi.org/10.1038/s41580-021-00415-0.
45. Wolin, M.S. Evidence for novel aspects of Nox4 oxidase regulation of mitochondrial function and peroxide generation in an endothelial cell model of senescence. *The Biochemical journal* **2013**, *452*, e1-2. https://doi.org/10.1042/bj20130484.
46. Okoye, C.N.; MacDonald-Jay, N.; Kamunde, C. Effects of bioenergetics, temperature and cadmium on liver mitochondria reactive oxygen species production and consumption. *Aquatic toxicology (Amsterdam, Netherlands)* **2019**, *214*, 105264. https://doi.org/10.1016/j.aquatox.2019.105264.
47. Adiele, R.C.; Stevens, D.; Kamunde, C. Differential inhibition of electron transport chain enzyme complexes by cadmium and calcium in isolated rainbow trout (Oncorhynchus mykiss) hepatic mitochondria. *Toxicological sciences : an official journal of the Society of Toxicology* **2012**, *127*, 110-119. https://doi.org/10.1093/toxsci/kfs091.
48. Bennett, C.F.; Latorre-Muro, P.; Puigserver, P. Mechanisms of mitochondrial respiratory adaptation. *Nature reviews. Molecular cell biology* **2022**, *23*, 817-835. https://doi.org/10.1038/s41580-022-00506-6.
49. Ge, J.; Zhang, C.; Sun, Y.C.; Zhang, Q.; Lv, M.W.; Guo, K.; Li, J.L. Cadmium exposure triggers mitochondrial dysfunction and oxidative stress in chicken (Gallus gallus) kidney via mitochondrial UPR inhibition and Nrf2-mediated antioxidant defense activation. *Sci Total Environ* **2019**, *689*, 1160-1171. https://doi.org/10.1016/j.scitotenv.2019.06.405.
50. Sun, M.; Jiang, Z.; Gu, P.; Guo, B.; Li, J.; Cheng, S.; Ba, Q.; Wang, H. Cadmium promotes colorectal cancer metastasis through EGFR/Akt/mTOR signaling cascade and dynamics. *Sci Total Environ* **2023**, *899*, 165699. https://doi.org/10.1016/j.scitotenv.2023.165699.

51. Dai, C.; Sharma, G.; Liu, G.; Shen, J.; Shao, B.; Hao, Z. Therapeutic detoxification of quercetin for aflatoxin B1-related toxicity: Roles of oxidative stress, inflammation, and metabolic enzymes. *Environmental pollution (Barking, Essex : 1987)* **2024**, *345*, 123474. https://doi.org/10.1016/j.envpol.2024.123474.
52. Green, D.R.; Reed, J.C. Mitochondria and apoptosis. *Science (New York, N.Y.)* **1998**, *281*, 1309-1312. https://doi.org/10.1126/science.281.5381.1309.
53. Mashimo, M.; Onishi, M.; Uno, A.; Tanimichi, A.; Nobeyama, A.; Mori, M.; Yamada, S.; Negi, S.; Bu, X.; Kato, J.; et al. The 89-kDa PARP1 cleavage fragment serves as a cytoplasmic PAR carrier to induce AIF-mediated apoptosis. *J Biol Chem* **2021**, *296*, 100046. https://doi.org/10.1074/jbc.RA120.014479.
54. Bello, M.; Morales-González, J.A. Molecular recognition between potential natural inhibitors of the Keap1-Nrf2 complex. *International journal of biological macromolecules* **2017**, *105*, 981-992. https://doi.org/10.1016/j.ijbiomac.2017.07.117.
55. Zhang, X.; Liu, Y.; Shen, Z.; Wang, S.; Wu, C.; Liu, D.; Tang, S.; Dai, C. Osthole ameliorates myonecrosis caused by Clostridium perfringens type A infection in mice. *One Health Advances* **2023**, *1*, 27. https://doi.org/10.1186/s44280-023-00028-6.
56. Gao, M.; Li, C.; Xu, M.; Liu, Y.; Cong, M.; Liu, S. LncRNA MT1DP Aggravates Cadmium-Induced Oxidative Stress by Repressing the Function of Nrf2 and is Dependent on Interaction with miR-365. *Adv Sci (Weinh)* **2018**, *5*, 1800087. https://doi.org/10.1002/advs.201800087.
57. Ren, X.; Xu, Y.; Yu, Z.; Mu, C.; Liu, P.; Li, J. The role of Nrf2 in mitigating cadmium-induced oxidative stress of Marsupenaeus japonicus. *Environmental pollution (Barking, Essex : 1987)* **2021**, *269*, 116112. https://doi.org/10.1016/j.envpol.2020.116112.
58. Wang, Q.; Botchway, B.O.A.; Zhang, Y.; Liu, X. Ellagic acid activates the Keap1-Nrf2-ARE signaling pathway in improving Parkinson's disease: A review. *Biomed Pharmacother* **2022**, *156*, 113848. https://doi.org/10.1016/j.biopha.2022.113848.
59. Cao, X.; Fu, M.; Bi, R.; Zheng, X.; Fu, B.; Tian, S.; Liu, C.; Li, Q.; Liu, J. Cadmium induced BEAS-2B cells apoptosis and mitochondria damage via MAPK signaling pathway. *Chemosphere* **2021**, *263*, 128346. https://doi.org/10.1016/j.chemosphere.2020.128346.
60. Chen, L.; Liu, L.; Huang, S. Cadmium activates the mitogen-activated protein kinase (MAPK) pathway via induction of reactive oxygen species and inhibition of protein phosphatases 2A and 5. *Free radical biology & medicine* **2008**, *45*, 1035-1044. https://doi.org/10.1016/j.freeradbiomed.2008.07.011.
61. Chen, L.; Liu, L.; Luo, Y.; Huang, S. MAPK and mTOR pathways are involved in cadmium-induced neuronal apoptosis. *J Neurochem* **2008**, *105*, 251-261. https://doi.org/10.1111/j.1471-4159.2007.05133.x.
62. Liu, Y.; Chang, J.; Yang, C.; Zhang, T.; Chen, X.; Shi, R.; Liang, Y.; Xia, Q.; Ma, S. Genome-wide CRISPR-Cas9 screening in Bombyx mori reveals the toxicological mechanisms of environmental pollutants, fluoride and cadmium. *Journal of hazardous materials* **2021**, *410*, 124666. https://doi.org/10.1016/j.jhazmat.2020.124666.
63. Hu, Y.R.; Ma, H.; Zou, Z.Y.; He, K.; Xiao, Y.B.; Wang, Y.; Feng, M.; Ye, X.L.; Li, X.G. Activation of Akt and JNK/Nrf2/NQO1 pathway contributes to the protective effect of coptisine against AAPH-induced oxidative stress. *Biomed Pharmacother* **2017**, *85*, 313-322. https://doi.org/10.1016/j.biopha.2016.11.031.
64. Tasaki, M.; Umemura, T.; Maeda, M.; Ishii, Y.; Okamura, T.; Inoue, T.; Kuroiwa, Y.; Hirose, M.; Nishikawa, A. Safety assessment of ellagic acid, a food additive, in a subchronic toxicity study using F344 rats. *Food Chem Toxicol* **2008**, *46*, 1119-1124. https://doi.org/10.1016/j.fct.2007.10.043.
65. Heilman, J.; Andreux, P.; Tran, N.; Rinsch, C.; Blanco-Bose, W. Safety assessment of Urolithin A, a metabolite produced by the human gut microbiota upon dietary intake of plant derived ellagitannins and ellagic acid. *Food Chem Toxicol* **2017**, *108*, 289-297. https://doi.org/10.1016/j.fct.2017.07.050.
66. Ardah, M.T.; Bharathan, G.; Kitada, T.; Haque, M.E. Ellagic Acid Prevents Dopamine Neuron Degeneration from Oxidative Stress and Neuroinflammation in MPTP Model of Parkinson's Disease. *Biomolecules* **2020**, *10*. https://doi.org/10.3390/biom10111519.
67. Baluchnejadmojarad, T.; Rabiee, N.; Zabihnejad, S.; Roghani, M. Ellagic acid exerts protective effect in intrastriatal 6-hydroxydopamine rat model of Parkinson's disease: Possible involvement of ERβ/Nrf2/HO-1 signaling. *Brain Res* **2017**, *1662*, 23-30. https://doi.org/10.1016/j.brainres.2017.02.021.